Title

Genetic Dissection of a Supergene Implicates Tfap2a in Craniofacial Evolution of Threespine Sticklebacks

Journal

Genetics, 209(2)

ISSN

0016-6731

Authors

Erickson, Priscilla A
Baek, Jiyeon
Hart, James C
et al.

Publication Date

2018-06-01

DOI

10.1534/genetics.118.300760

Peer reviewed

Genetic Dissection of a Supergene Implicates *Tfap2a* in Craniofacial Evolution of Threespine Sticklebacks

Priscilla A. Erickson, Jiyeon Baek, James C. Hart, Phillip A. Cleves, and Craig T. Miller[1]
Department of Molecular and Cell Biology, University of California, Berkeley, California 94720
ORCID IDs: 0000-0001-8420-995X (P.A.E.); 0000-0002-6746-5086 (J.B.); 0000-0002-6245-0459 (J.C.H.); 0000-0002-8526-8940 (P.A.C.); 0000-0002-1970-8389 (C.T.M.)

ABSTRACT In nature, multiple adaptive phenotypes often coevolve and can be controlled by tightly linked genetic loci known as supergenes. Dissecting the genetic basis of these linked phenotypes is a major challenge in evolutionary genetics. Multiple freshwater populations of threespine stickleback fish (*Gasterosteus aculeatus*) have convergently evolved two constructive craniofacial traits, longer branchial bones and increased pharyngeal tooth number, likely as adaptations to dietary differences between marine and freshwater environments. Prior QTL mapping showed that both traits are partially controlled by overlapping genomic regions on chromosome 21 and that a regulatory change in *Bmp6* likely underlies the tooth number QTL. Here, we mapped the branchial bone length QTL to a 155 kb, eight-gene interval tightly linked to, but excluding the coding regions of *Bmp6* and containing the candidate gene *Tfap2a*. Further recombinant mapping revealed this bone length QTL is separable into at least two loci. During embryonic and larval development, *Tfap2a* was expressed in the branchial bone primordia, where allele specific expression assays revealed the freshwater allele of *Tfap2a* was expressed at lower levels relative to the marine allele in hybrid fish. Induced loss-of-function mutations in *Tfap2a* revealed an essential role in stickleback craniofacial development and show that bone length is sensitive to *Tfap2a* dosage in heterozygotes. Combined, these results suggest that closely linked but genetically separable changes in *Bmp6* and *Tfap2a* contribute to a supergene underlying evolved skeletal gain in multiple freshwater stickleback populations.

KEYWORDS QTL; fine mapping; skeletal evolution; genome editing; supergene

INTRASPECIFIC morphological variation offers the opportunity to dissect the genetic changes that underlie evolution, including adaptation to novel environments. Genetic mapping studies of naturally varying traits can reveal the genomic regions that contribute to evolutionary changes. When multiple phenotypes are controlled by the same region of a genome, a single pleiotropic locus could affect multiple traits, or separate but closely linked genes could affect each trait independently. Clustering of two or more QTL into supergenes is a commonly described feature of evolution (Schwander *et al.* 2014; Thompson and Jiggins 2014), likely because close linkage of loci allows advantageous combinations of traits to be inherited together. Supergenes have been shown to control pigmentation patterns in locusts (Nabours 1933); mimetic patterns in butterflies (Joron *et al.* 2011; Kunte *et al.* 2014); color and patterning in snails (Murray and Clarke 1976a,b); social behavior in ants (Wang *et al.* 2013; Pracana *et al.* 2017); breeding behavior, morphology, and sperm traits in birds (Thomas *et al.* 2008; Küpper *et al.* 2016; Lamichhaney *et al.* 2016; Tuttle *et al.* 2016; Kim *et al.* 2017); and life history, morphology, and pollination syndromes in plants (Mather 1950; Lowry and Willis 2010; Hermann *et al.* 2013). The supergenes that have been molecularly characterized to date are often controlled by chromosomal inversions with large phenotypic effects. In *Heliconius* butterflies, a supergene in one species was shown to be an inversion containing tightly linked loci that can recombine in other species (Joron *et al.* 2006, 2011; Nadeau *et al.* 2016). Determining whether clustering of QTL controlling different traits is caused by close linkage or pleiotropy requires careful genetic dissection of the genomic intervals of interest.

doi: https://doi.org/10.1534/genetics.118.300760
Manuscript received January 26, 2018; accepted for publication March 26, 2018; published Early Online March 28, 2018.
Supplemental material available at Figshare: https://doi.org/10.25386/genetics.6024338.
[1]Corresponding author: Department of Molecular and Cell Biology, 142 Life Sciences Addition #3200, University of California, Berkeley, Berkeley, CA 94720. E-mail: ctmiller@berkeley.edu

While QTL for different traits can cluster in the genome, multiple genetic changes affecting a single phenotype can also be clustered within a QTL. Whether a given QTL typically represents an individual locus, or alternatively, multiple tightly linked loci, remains a largely open question in quantitative genetics. For example, QTL mapping in maize × teosinte crosses has revealed that some large-effect QTL can fractionate (Studer and Doebley 2011), including a QTL that was fractionated into up to five distinct tightly linked loci (Lemmon and Doebley 2014). In contrast, other maize × teosinte QTL contain single causative loci (Wang *et al.* 2005; Hung *et al.* 2012; Wills *et al.* 2013). In mice, one QTL controlling pigmentation maps to a single coding mutation in *Mc1r* (Steiner *et al.* 2007), but a second QTL maps to multiple smaller effect mutations affecting different aspects of *Agouti* expression (Linnen *et al.* 2013). Interspecific differences in *Drosophila* pigmentation map, in part, to a single regulatory element of *tan* (Jeong *et al.* 2008) and multiple point mutations in a single enhancer of *ebony* (Rebeiz *et al.* 2009), but differences in *Drosophila* trichome patterning are caused by changes in regulatory elements of the *shavenbaby* gene that are spread over 50 kb (McGregor *et al.* 2007; Frankel *et al.* 2011).

Testing whether the same or different genetic changes underlie the evolution of similar phenotypes in multiple lineages may shed light on the predictability and repeatability of evolution (Stern and Orgogozo 2008; Stern 2013; Rosenblum *et al.* 2014). Both theoretical and empirical studies indicate that parallel genetic evolution can occur quite often (Orr 2005; Conte *et al.* 2012). However, given the relatively small number of cases where convergently evolved phenotypes have been associated with specific genes, the extent of genetic parallelism remains largely unknown, especially for quantitative traits.

The threespine stickleback fish has convergently evolved countless freshwater forms from ancestral marine populations and has emerged as a powerful model system for studying both the genetic basis and repeatability of morphological evolution (Peichel and Marques 2017). In freshwater environments, sticklebacks repeatedly evolve a suite of craniofacial and other morphological adaptations to cope with differences in diet, predation, and other environmental variables (Bell and Foster 1994). Individuals from different populations are easily intercrossed to produce large clutches in the laboratory (Peichel *et al.* 2001), the stickleback genome is well assembled and annotated (Jones *et al.* 2012; Glazer *et al.* 2015), and reverse genetic techniques are available (Erickson *et al.* 2016a), facilitating both genetic and genomic dissection of the molecular basis of evolved traits.

Marine and freshwater sticklebacks occupy different trophic niches: while marine fish feed on small planktonic prey, freshwater fish typically consume diets of larger macroinvertebrates (Kislalioglu and Gibson 1977; Gross and Anderson 1984). Sticklebacks process food primarily in the throat, with the branchial skeleton and pharyngeal jaw used to chew and crush food en route to the gut (McGee and Wainwright 2013; McGee *et al.* 2013). The branchial skeleton forms in the posterior-most five pharyngeal arches and consists of segmental homologs of the upper and lower jaw. The branchial skeleton is composed of five bilateral pairs of ventral bones (ceratobranchials), four bilateral pairs of dorsal bones (epibranchials), and three bilateral pairs of tooth plates (Anker 1974; see Supplemental Material, Figure S1 for anatomy). We described increases in both pharyngeal tooth number and branchial bone length as repeatable and heritable features of freshwater adaptation (Cleves *et al.* 2014; Erickson *et al.* 2014; Ellis *et al.* 2015). We hypothesize that these increases permit freshwater fish to eat larger prey items via a larger pharyngeal cavity and greater chewing capacity. The first epibranchial (EB1) bone, a serial homolog of the upper jaw, serves as a critical lever for the mastication motion of the pharyngeal jaw (Wainwright 2006) and is the most proportionally elongated branchial bone in freshwater sticklebacks (Erickson *et al.* 2014). The branchial bones are endochondral bones that form from cartilage templates during late embryonic development (Haines 1934), much like mammalian long bones (Haines 1942). Changes to both the early patterning of cartilage and the relative growth of bones contribute to stickleback branchial bone length differences (Erickson *et al.* 2014) and to skeletal evolution in other systems (Farnum *et al.* 2008a,b; Sanger *et al.* 2011, 2012).

Previous genetic mapping of evolved stickleback skeletal variation has identified >100 QTL controlling a variety of traits, including pharyngeal tooth number and branchial bone length, in the benthic population from Paxton Lake, British Columbia (PAXB). These trophic traits are highly polygenic, but the QTL controlling skeletal adaptation are significantly clustered into supergenes on three chromosomes, including chromosome 21 (Miller *et al.* 2014). Although chromosome 21 contains an inversion that typically differs between marine and freshwater populations (Jones *et al.* 2012), the PAXB pharyngeal tooth number QTL was fine-mapped to a genomic region over 1 Mb outside this inversion, to an intronic enhancer of the gene *Bone morphogenetic protein 6* (*Bmp6*) (Cleves *et al.* 2014; P. Cleves, J. Hart, R. Agoglia, M. Jimenez, P. Erickson, L. Gai, and C. Miller, unpublished data 2018). Additional work mapped branchial bone length QTL to peaks near *Bmp6* on chromosome 21 in both PAXB and a stream population from Fishtrap Creek, Washington (FTC) (Erickson *et al.* 2014). BMP ligands are critical for both tooth and bone development (Balic and Thesleff 2015; Salazar *et al.* 2016), so *Bmp6* is an excellent candidate gene for both the tooth number and branchial bone length QTL. However, a second excellent candidate gene for the branchial bone length QTL, *Tfap2a*, a known regulator of pharyngeal skeletal development (Schorle *et al.* 1996; Knight *et al.* 2004; Milunsky *et al.* 2008; Tekin *et al.* 2009; Van Otterloo *et al.* 2018), is tightly linked to *Bmp6*. We sought to further elucidate the genetic basis of the increased bone length QTL in both the FTC and PAXB freshwater populations to answer three questions: (1) Are the bone length and tooth number QTL genetically separable? (2) What is the developmental genetic basis of the bone length QTL? and

(3) Does convergent evolution of branchial bone gain in two freshwater populations have a similar genetic basis?

Materials and Methods

Animal statement

All animal work was approved by University of California, Berkeley (animal protocol #R330). Fish were reared as previously described (Erickson *et al.* 2014).

Recombinant mapping and statistical analysis

Fish segregating for the chromosome 21 EB1 length QTL from the PAXB × Little Campbell Marine (LITC) and FTC × LITC crosses (Erickson *et al.* 2014) were propagated and genotyped with markers Stn487 (Cleves *et al.* 2014), PAE309, PAE323, and/or PAE349 (Table S1) to ensure that marine and freshwater alleles of the QTL interval were passed on to each generation and to look for recombination events within the QTL interval. To test the phenotypic effects of recombinant chromosomes, recombinant fish were crossed to related fish that were either heterozygous for the QTL or homozygous for the marine chromosome within the QTL interval. Offspring were grown to 25–28 days postfertilization (dpf) (10–12 mm, FTC cross) or to roughly 80 dpf (∼20 mm, PAXB cross). These fish were fixed, stained with Alizarin red, cleared, dissected, and photographed, and EB1 bone length was measured as previously described, using ImageJ (Erickson *et al.* 2014; Miller *et al.* 2014; Ellis and Miller 2016). EB1 length was measured on both the left and right side and averaged. Bone length was corrected for fish standard length in each clutch separately and residuals of bone length or back-transformed residuals were used for all analyses. Pharyngeal tooth number was counted as described (Cleves *et al.* 2014).

For recombinant fish crossed to heterozygotes, the R package *lmtest* was used to perform a likelihood ratio test (*lrtest*) to determine whether the recombinant chromosome behaved as marine or freshwater. The recombinant chromosome (R) was coded as either (*a*) a marine (M) or (*b*) a freshwater (F) chromosome. For (*a*), the MR and FR genotypes were replaced with MM and MF, respectively, and for (*b*), they were replaced with MF and FF. The genotypes were then coded numerically with MM = 0, MF = 1, and FF = 2. The *lrtest* function was used to compare two nested linear models of bone length: the model (*bone length* $\sim a + b$) was compared to the model (*bone length* $\sim a$) and to the model (*bone length* $\sim b$). A significant difference between the model containing both possible genotypes and a model containing one possible genotype indicated that the addition of the second genotype significantly improved the fit of the model, and therefore that the second genotype best represented the effect of the recombinant chromosome. For example, a significant *P*–value in the likelihood ratio test comparing (*bone length* $\sim a + b$) to (*bone length* $\sim a$) would indicate that the addition of *b* significantly improved the model and therefore that R behaves as F. For recombinant chromosomes crossed to homozygous marine fish (MM), a *t*-test was used to determine whether the recombinant chromosome behaved like a freshwater chromosome (*i.e.*, there was a significant increase in bone length between the MM and MR genotypic classes).

Analysis of chromosome 21 QTL in previously published crosses

Genotype data from Glazer *et al.* (2015) and Erickson *et al.* (2016b) were used to test for the presence of a bone length QTL at the genotype-by-sequencing (GBS) marker containing *Tfap2a* (binned marker 16_9) in the LITC × FTC (a different cross than the FTC cross presented here) and LITC × Enos Benthic (ENOB) crosses. Adult bone lengths were measured for 210 fish from the three largest families in the Glazer *et al.* (2015) study as described above, and processed to correct for size and sex as described in Erickson *et al.* (2016b). Processed adult bone lengths for the ENOB × LITC cross were used as reported in Erickson *et al.* (2016b).

Genome resequencing and Tfap2a genotyping

A synonymous polymorphism in *Tfap2a* was initially identified by examining the genome sequences of the grandparents of a previously studied LITC × FTC cross (a different cross than the one studied here; Glazer *et al.* 2015) and a PAXB × LITC cross (the same cross as the one studied here; P. Cleves, J. Hart, R. Agoglia, M. Jimenez, P. Erickson, L. Gai, and C. Miller, unpublished data). This mutation (see Figure S2 for location) disrupts an *Ava*I cut site and was genotyped by amplifying with PAE414/416 (Table S1) and digesting the PCR product with *Ava*I; presence of an uncut band indicated presence of the freshwater alternate allele.

Allele-specific expression assay for Tfap2a

We modified a GBS protocol (Elshire *et al.* 2011; Glazer *et al.* 2015) to assay allele-specific expression (ASE) in RT-PCR products amplified from complementary DNA (cDNA) relative to genomic DNA (gDNA) PCR controls. PAXB × LITC fish segregating marine and freshwater alleles of the QTL interval (F9 generation) were intercrossed, their F10 larval offspring were euthanized with MS-222, and the branchial skeleton or EB1 was immediately dissected on ice and stored in 500 μl TRI reagent (Ambion) at −80°. Tissue was collected from five time points: 9, 13, 17, 22, and 35 dpf. At 9 and 13 dpf, the entire branchial skeleton was collected. At 17 and 22 dpf, the dorsal portion of the branchial skeleton was collected, and at 35 dpf individual EB1 bones were isolated. The remaining tissue was stored in ethanol. DNA was isolated from the excess tissue by digesting overnight with Proteinase K in lysis buffer at 55° and then performing a phenol-chloroform extraction followed by ethanol precipitation (Green and Sambrook 2012). DNA was genotyped with indel marker PAE311/312 (Table S1) to identify heterozygous fish. RNA was extracted from heterozygous fish following the TRI reagent manufacturer's protocol, with the final RNA pellet resuspended in 20 μl RNase free water. For each time point, 24 fish were collected, yielding ∼12 heterozygotes.

To prepare cDNA, 4.5 μl RNA was treated with 0.5 μl amplification grade DNase I (Invitrogen, Carlsbad, CA) according to the manufacturer's protocol. cDNA was synthesized with Superscript III (Invitrogen), using random hexamers according to the manufacturer's protocol but halving all volumes to produce a final volume of 10 μl cDNA. One microliter of cDNA or 50 ng of gDNA from each fish was used as template in separate Phusion PCR reactions with primers PAE414 and PAE416 (Table S1), designed to amplify the synonymous SNP in *Tfap2a* at position chrXXI:4,265,995, which was shared in both the PAXB and FTC cross parents. The 5′ end of each primer contained an *Ape*KI cut site so that the product could be ligated into the GBS adapters. A titration control was performed by mixing marine and freshwater DNA in fixed ratios. Technical replicates were performed by (1) amplifying the same gDNA twice, (2) preparing cDNA from the same RNA sample twice, and (3) amplifying from the same cDNA sample twice. All PCR products were purified in a 96-well format by the University of California, Berkeley DNA Sequencing Facility and quantified using a PicoGreen assay (ThermoFisher) on a BioTek Flx800 plate reader.

Up to 25 ng of each purified PCR product was used in the GBS library preparation as previously described (Elshire *et al.* 2011; Glazer *et al.* 2015). Briefly, the PCR products were combined with 1.8 ng of barcoded adapters and digested with *Ape*KI (New England BioLabs, Ipswich, MA) for 2 hr at 75°. The adapters were ligated to the PCR products with T4 DNA Ligase (New England BioLabs) for 1 hr at 22°. Then, 5 μl of each ligation product was pooled for a PCR purification (Qiagen, Valencia, CA). Sequencing adapters were added with 10 cycles of PCR using Taq 2× master mix (New England BioLabs). The PCR product was cleaned up and size-selected twice with 1.5 vol of Sera-Mag beads prepared as previously described (Rohland and Reich 2012). Six libraries were pooled equally into one Illumina HiSequation 2000 lane and sequenced on 50 bp single-end rapid run mode at the University of California, Berkeley Vincent J. Coates Genomic Sequencing Laboratory. Indexed and barcoded sequences were demultiplexed and aligned to the expected PCR product sequence to count marine and freshwater alleles at the polymorphic site with the custom script *nuc_by_pos.py* (available at https://github.com/trahsemaj/TFAP2). Samples receiving <300 aligned reads were removed from the analysis ($n = 4$), as preliminary experiments suggested that at least 300 reads would be required to obtain reliable 1:1 allelic ratios for gDNA PCR products. Outliers >3 SD from the mean were also removed ($n = 2$). The gDNA and cDNA freshwater/marine ratios were compared at each time point to test for ASE with a Mann–Whitney *U*-test using the *wilcox.test* function in R.

Genome editing of Tfap2a

TALENs were generated to target the second exon of *Tfap2a* (see Table S2 for RVD design and Figure S2 for binding sites) following established protocols (Cermak *et al.* 2011; Doyle *et al.* 2012) and injected into one-cell FTC and LITC stickleback embryos as previously described (Erickson *et al.* 2015, 2016a). A subset of injected embryos ($n = 10$–12) were screened for mutations by amplifying with primers PAE379 and PAE381 (Table S1) in a standard Phusion (New England BioLabs) reaction, digesting the PCR product with *Pvu*II, and running the digested product on a 1% agarose gel. Undigested product of ~297 bp indicated molecular lesions that disrupted a *Pvu*II sequence at the expected DNA cleavage site. Clutches carrying lesions were raised to adulthood and outcrossed to wild-type fish. Lesions were sequenced by extracting the undigested PCR band from an agarose gel followed by Sanger sequencing (see Table S3 for lesions studied). F1 fish carrying lesions were propagated for further analysis.

TALEN phenotyping

Tfap2a$^{+/-}$ heterozygotes were intercrossed to produce clutches containing homozygous mutants. These larval fish were euthanized immediately after hatching (9–10 dpf), fixed overnight in 4% paraformaldehyde in 1× PBS, stained with Alcian blue, digested with trypsin, mounted in glycerol (Kimmel *et al.* 1998), and imaged on a Leica DM2500 compound microscope. For bone length phenotyping, heterozygous fish were outcrossed to wild-type laboratory-reared individuals. In the FTC background, a total of 144 fish were studied from three families carrying a 16 bp insertion, an 8 bp deletion, and a 10 bp deletion. In LITC, two families totaling 96 fish carrying a 13 bp deletion were studied. Fish were raised to 25–28 dpf and genotyped and phenotyped as described above. Bone lengths were not back-transformed in this analysis due to different standard length ranges and different *y*-intercepts of the bone length ~ standard length regression for fish in different families.

In situ hybridization

In situ hybridization for *Tfap2a* was performed on whole embryos as previously described (Cleves *et al.* 2014).

Data and reagent availability

Raw data used in this study including genotypes, phenotypes, and ASE counts are available in File S1. Supplemental material is available at Figshare: https://doi.org/10.25386/genetics.6024338. All reagents used are available upon request. Custom Python script used for ASE is available at https://github.com/trahsemaj/TFAP2.

Results

Fine mapping the chromosome 21 bone length QTL

We tested whether bone length and tooth number were controlled by the same genomic region in two freshwater × marine crosses known to carry the bone length QTL (Erickson *et al.* 2014): PAXB and FTC, both crossed to LITC. We analyzed a series of recombinant chromosomes derived from later generations of the original crosses. For each recombinant chromosome, we used likelihood ratio tests to

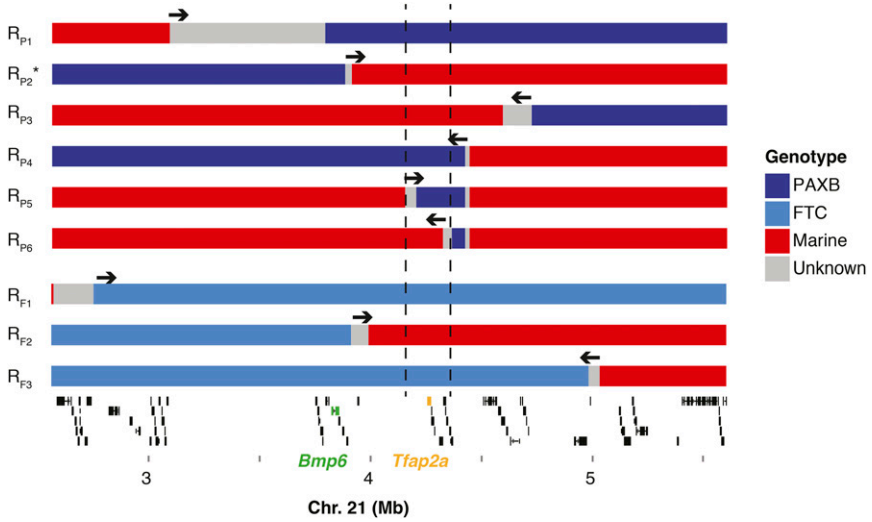

Figure 1 Recombinant mapping of the chromosome 21 bone length QTL in two crosses. Recombinant chromosomes were identified in later generations (>F4) of the original F2 crosses described in Erickson *et al.* (2014). Fish with recombinant chromosomes were crossed to known genotype relatives descended from the same cross. Colors indicate the marine/freshwater identity along each recombinant chromosome; regions of unknown genotype between confirmed breakpoint genotypes are colored gray (see key). Arrows above each chromosome indicate the direction of the bone length QTL relative to the recombination break point; see Table 1 for full statistical analysis of each cross. Note that recombinant chromosomes R_{P5} and R_{P6} in the PAXB cross are both double recombinants derived from chromosome R_{P4}. The asterisk on R_{P2} indicates that this chromosome also carries a tooth number QTL (P. Cleves, J. Hart, R. Agoglia, M. Jimenez, P. Erickson, L. Gai, and C. Miller, unpublished data). The vertical dashed lines indicate the boundaries of the fine-mapped region in the PAXB × LITC cross. An Ensembl-based gene prediction track from the stickleback genome (chrXXI: 2.56–5.60 Mb) is shown below (Jones *et al.* 2012). Thick lines indicate predicted exons and thin lines indicate introns. *Bmp6* and *Tfap2a* are highlighted in green and yellow, respectively.

ask whether the recombinant chromosome produced a phenotypic effect significantly more similar to a marine or freshwater chromosome. If the chromosome behaved like a freshwater chromosome (significantly increased branchial bone length relative to a marine chromosome or did not differ from a freshwater chromosome), we concluded that the QTL was contained within the freshwater portion of the recombinant chromosome (blue in Figure 1). If the chromosome behaved like a marine chromosome (did not increase branchial bone length relative to a marine chromosome or caused significantly shorter bone length when compared to a freshwater chromosome), we concluded that the QTL was contained within the marine portion (red in Figure 1).

Using this approach, we identified recombinant chromosomes in each cross with recombination events located within ~2 Mb of *Bmp6*. In the PAXB cross, we identified one recombinant chromosome that separated the *Bmp6* locus from the region controlling bone length (Figure 1, chromosome R_{P2}). This particular recombinant chromosome significantly increases pharyngeal tooth number (P. Cleves, J. Hart, R. Agoglia, M. Jimenez, P. Erickson, L. Gai, and C. Miller, unpublished data), but did not significantly affect the length of the EB1 bone (Table 1). Therefore, bone length and tooth number are controlled by different genetic loci on chromosome 21 in the PAXB × LITC cross. In the FTC cross, we also found a chromosome that carried a freshwater allele of *Bmp6* but did not affect bone length (Figure 1, chromosome R_{F2} and Table 1). We found that this recombinant chromosome increased pharyngeal tooth number relative to a marine chromosome (Figure S3), suggesting that the FTC population also harbors a tooth QTL in a portion of the chromosome containing *Bmp6*, and like in the PAXB population, the regions controlling tooth number and bone length are genetically separable. The coding sequence of *Bmp6* is excluded from the bone length QTL interval in both crosses.

With subsequent fine mapping, we narrowed the QTL interval in the PAXB cross (Figure 1 and Table 1). Notably, a double recombinant chromosome in the PAXB cross (chromosome R_{P5}) shows no phenotypic difference from the original recombinant chromosome (R_{P4}), which had a strong effect on bone length (Table 1), suggesting that the freshwater alleles within the double recombinant region are sufficient to increase bone length. A second double recombinant sharing the same 3′ breakpoint (recombinant R_{P6}) did not differ from a marine chromosome, suggesting that this smaller freshwater portion of the chromosome does not carry the bone length QTL. Combined, these two results map the bone length QTL to a 155 kb region (chrXXI:4,200,364–4,355,895) in the PAXB cross, containing eight Ensembl-predicted genes (*Tfap2a*, *Tmem14b*, *Mak*, *Plcxd2*, *Phldb2*, *Tmem56*, *ENSGACG00000002373*, and *Bco1*; Jones *et al.* 2012. Seven of these eight genes have no described roles in mouse skeletal development (Smith *et al.* 2014). However, one gene, *Transcription Factor Activating Protein 2 alpha* (*Tfap2a*), is an outstanding candidate for craniofacial evolution because it has roles in patterning the craniofacial skeleton in humans, mice, and zebrafish (Schorle *et al.* 1996; Knight *et al.* 2004; Milunsky *et al.* 2008), and in regulating the growth and maturation of mammalian chondrocytes (Wenke and Bosserhoff 2010).

Fine mapping the bone length QTL in the FTC cross supported a larger ~1.1 Mb genomic interval (chrXXI: 3,906,104–5,003,790 bp; Figure 1 and Table 1), also containing *Tfap2a*. The entire PAXB fine-mapped interval is contained within the FTC fine-mapped interval. Therefore, together these data support a model of a shared genomic basis for branchial bone length gain in these two independently derived freshwater populations.

Table 1 Statistical analysis of recombinant chromosomes

Name	Cross	Design	Generation	*N*	Clutches	Geno 1	Geno 2	Geno 3	Geno 4	LR test (M)	LR test (F)	*t*-test	Conclusion (Mb)
R_{P1}	PAXB × LITC	MR × MM	F7	125	3	MM (−4.7 ± 21.2)	MR (5.6 ± 21.1)	—	—	—	—	**0.008**	right of 3.09
R_{P2}	PAXB × LITC	MR × MM	F7	96	2	MM (1.5 ± 15.8)	MR (−1.2 ± 17.7)	—	—	—	—	0.43	right of 3.88
R_{P3}	PAXB × LITC	MR × MF	F6	192	2	MM (−3.4 ± 27.8)	MR (−10.4 ± 25)	MF (2.6 ± 22.2)	FR (9.3 ± 29.0)	**0.04**	0.99	—	left of 4.89
R_{P4}	PAXB × LITC	MR × MF	F6	171	2	MM (−10.4 ± 20.1)	MR (3.1 ± 30.9)	MF (0.4 ± 23.4)	FR (8.6 ± 25.2)	0.59	**0.005**	—	left of 4.4
R_{P5}	PAXB × LITC	$R_{P4}R_{P5}$ × MM	F8	62	1	MR_{P5} (4.6 ± 23.9)	MR_{P4} (−4.4 ± 32.5)	—	—	—	—	0.22	between 4.15–4.44
R_{P6}	PAXB × LITC	MR × MM	F9	78	1	MM (4.2 ± 28.2)	MR (1.9 ± 28.0)	—	—	—	—	0.72	excludes 4.32–4.44
R_{F1}	FTC × LITC	FR × MF	F8	96	2	MR (−7.4 ± 9.7)	MF (−5.5 ± 11.4)	FR (5.6 ± 8.9)	FF (9.3 ± 10.3)	0.22	**0.0002**	—	right of 2.57
R_{F2}	FTC × LITC	MR × MM	F8	76	2	MM (−2.0 ± 11.8)	MR (1.0 ± 10.0)	—	—	—	—	0.25	right of 3.91
R_{F3}	FTC × LITC	FR × MF	F8	63	1	MR (−11.8 ± 10.3)	MR (1.7 ± 13.3)	MF (1.8 ± 12.9)	FR (11.3 ± 13.5)	0.93	**0.0004**	—	left of 5.03

Each row corresponds to one chromosome in Figure 1 (in order from top to bottom). All bone length measurements were size-corrected within individual clutches and then pooled. Reported values for each genotypic class are mean residual bone lengths (in micrometer) ± SD. *P*-values for linear model likelihood ratio (LR) tests or *t*-tests are reported when appropriate and bolded when significant; see *Materials and Methods* for details on the statistical tests. Arrows in Figure 1 indicate the conclusion for each chromosome. M, marine; F, freshwater; R, recombinant.

Fractionation of the QTL in the FTC cross

For one FTC recombinant chromosome, we found evidence of fractionation of the bone length QTL. The breakpoint of this recombinant was within a large (~200 kb) gene desert between *Bmp6* and *Tfap2a* (Figure 2A). We compared the effect of this recombinant chromosome to both marine and freshwater chromosomes that were nonrecombinant within the QTL region. We found that this recombinant chromosome produced significantly longer bones than a marine chromosome (Figure 2B); however, it also produced significantly shorter bones than a freshwater chromosome (Figure 2C). These data suggest the recombinant chromosome has effects intermediate between fully marine and freshwater alleles, and the freshwater portion of this chromosome does not recapitulate the full QTL effect.

Variable presence of the chromosome 21 bone length QTL in freshwater populations

We previously reported a relatively weak EB1 bone length QTL at the far end of chromosome 21 (41.7 cM away from *Tfap2a*) in a LITC × ENOB cross (Erickson *et al.* 2016b), but in this cross there is no association between *Tfap2a* genotype and EB1 length (Figure S4A). Additionally, a LITC × FTC cross with different grandparents than those used in the present study (Glazer *et al.* 2014, 2015) also shows no evidence for a bone length QTL near *Tfap2a* (Figure S4B). Therefore, while this bone length QTL was identified in two populations, it appears to not be present in all freshwater populations nor fixed in the FTC population. These cases where this bone length QTL was not detected could reflect differences in genetic background that mask the penetrance of the QTL, or alternatively, a true absence of the mutation(s) underlying the QTL.

The chromosome 21 QTL affects bone length at stages soon after ossification

Our previous findings that cartilage template size was larger and bone growth rate was accelerated in the FTC population (Erickson *et al.* 2014) raised the question of whether the chromosome 21 QTL controlled cartilage development, bone development, or both. To address this question, we raised F5 fish from the FTC × LITC cross to 13 days dpf (a stage when the EB1 cartilage template has formed but not ossified) and 20 dpf (a stage soon after EB1 ossification) to test for an effect of the chromosome 21 QTL on cartilage and bone length. The QTL did not have a significant effect on EB1 cartilage length in a heterozygous × marine backcross at 13 dpf, but had a strong effect on bone length by 20 dpf (Figure S5). Therefore, the chromosome 21 QTL likely has an effect on either initial bone ossification or bone elongation, but does not appear to have a substantial effect on EB1 cartilage template length.

Expression of Tfap2a in developing branchial skeletons

We previously showed that *Tfap2a* is expressed in undifferentiated mesenchymal cells in the dorsal branchial skeletal

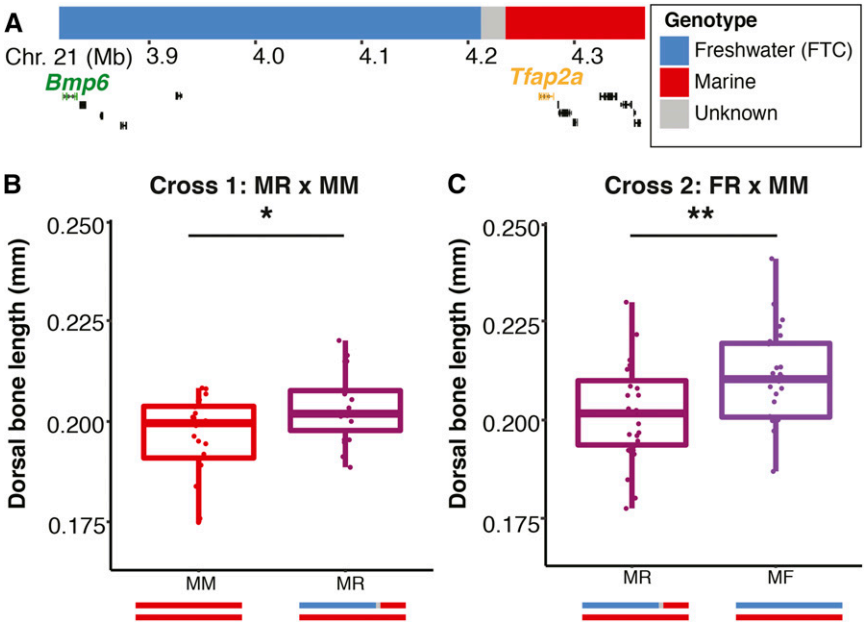

Figure 2 Fractionation of the bone length QTL in the FTC × LITC cross. A single recombinant chromosome with breakpoint between 4,210,854 and 4,231,226 bp (A) was identified and then bred to produce fish with genotypes MR and FR (M, marine; F, freshwater; R, recombinant). Note this chromosome is distinct from those shown in Figure 1. The Ensembl gene predictions for this region (chrXXI: 3.85–4.35 Mb) are shown below with *Bmp6* and *Tfap2a* highlighted (Jones *et al.* 2012). Each genotype was crossed to an MM fish (homozygous for marine genotypes on chromosome 21) and epibranchial one bone length (size-corrected and back transformed to a 9 mm fish) was compared between genotypes in each cross. The recombinant chromosome diagrammed in A results in bones significantly longer than those from an M chromosome (B) (*t*-test: d.f. = 38.98, $t = -2.51$, $P = 0.017$) but significantly shorter than those from an F chromosome (C) (*t*-test: d.f. = 49.13, $t = 2.75$, $P = 0.008$). Schematics depicting the genotypes of the offspring are illustrated below the *x*-axes in B and C. * $P < 0.05$; ** $P < 0.001$.

primordia prior to epibranchial chondrification, but not in developing teeth (Cleves *et al.* 2014). To further characterize the temporal emergence of this dorsal branchial expression domain, we assayed *Tfap2a* expression at earlier stages in development. At 4 dpf, *Tfap2a* was broadly expressed in postmigratory cranial neural crest in the posterior pharyngeal arches (Figure 3, A and B). By 5 dpf, expression was detected in postmigratory cranial neural crest in the dorsal pharyngeal arches (Figure 3C). At 7 dpf, as previously reported, expression was detected in undifferentiated mesenchymal cells in the dorsal branchial arches, in precisely the future locations of the epibranchial cartilages (Figure 3, D–F). Thus, *Tfap2a* expression during craniofacial development is found in the right place and right time to regulate branchial bone development, further supporting *Tfap2a* as contributing to the branchial bone length QTL. We detected no obvious qualitative differences in expression patterns or levels between marine and freshwater embryos.

Evolved changes in the cis-regulation of Tfap2a

We first tested for coding changes in *Tfap2a* with genome resequencing data of a FTC grandparent from a previous study (Glazer *et al.* 2015) and the PAXB grandparent used in this study (P. Cleves, J. Hart, R. Agoglia, M. Jimenez, P. Erickson, L. Gai, and C. Miller, unpublished data). We identified a silent mutation shared between PAXB and FTC and an additional silent mutation in PAXB, but no nonsynonymous changes. Since no predicted protein coding changes exist in either freshwater population, we next tested for *cis*-regulatory differences in *Tfap2a*.

We compared the ratios of expressed marine (LITC) and freshwater (PAXB) alleles of *Tfap2a* in developing branchial skeletal tissue of marine × freshwater hybrid fish to look for allele-specific expression (ASE) (Cowles *et al.* 2002; Yan *et al.* 2002; Wittkopp *et al.* 2004). We adapted a barcoded next-generation sequencing assay originally developed for GBS (Elshire *et al.* 2011; Glazer *et al.* 2015) and verified that this assay is capable of detecting a range of allelic ratios despite some inherent variability (Figure S6). We tested a series of developmental stages of PAXB × LITC F9 hybrids for ASE of *Tfap2a*. The earliest stage collected for ASE was hatching (9 dpf), when the branchial skeleton could be accurately dissected. We collected additional time points at 13 and 17 dpf (immediately before ossification of EB1), 22 dpf (immediately following ossification of EB1), and 35 dpf (during growth of EB1). We compared the freshwater/marine allelic ratio of RT-PCR products amplified from cDNA to that of PCR products amplified from gDNA controls (which should have a ratio of 1:1 in heterozygous fish). While the observed allelic ratios have a high variance and only one developmental stage showed a significant difference between the gDNA ratio and the cDNA ratio, at every stage the median expression of the freshwater allele was lower than the marine allele (Figure 4). When the data from all five stages were pooled, the measured freshwater/marine allelic ratio was significantly reduced in cDNA samples relative to gDNA controls ($P = 0.001$, Mann–Whitney U, Figure 4). These findings reveal that *Tfap2a* has evolved *cis*-regulatory changes and further suggest that *Tfap2a* might have an inhibitory role in bone development, as reduction of expression of the freshwater allele of *Tfap2a* is associated with longer bones.

Tfap2a dosage affects branchial bone length and craniofacial development

Based on the results of the fine mapping and ASE assays, we hypothesized that manipulation of *Tfap2a* levels could affect branchial bone length. We used TALENs to induce predicted loss-of-function mutations (see Table S3) in *Tfap2a* in the FTC and LITC genetic backgrounds. We intercrossed stable heterozygous mutants to produce *trans*-heterozygotes. As

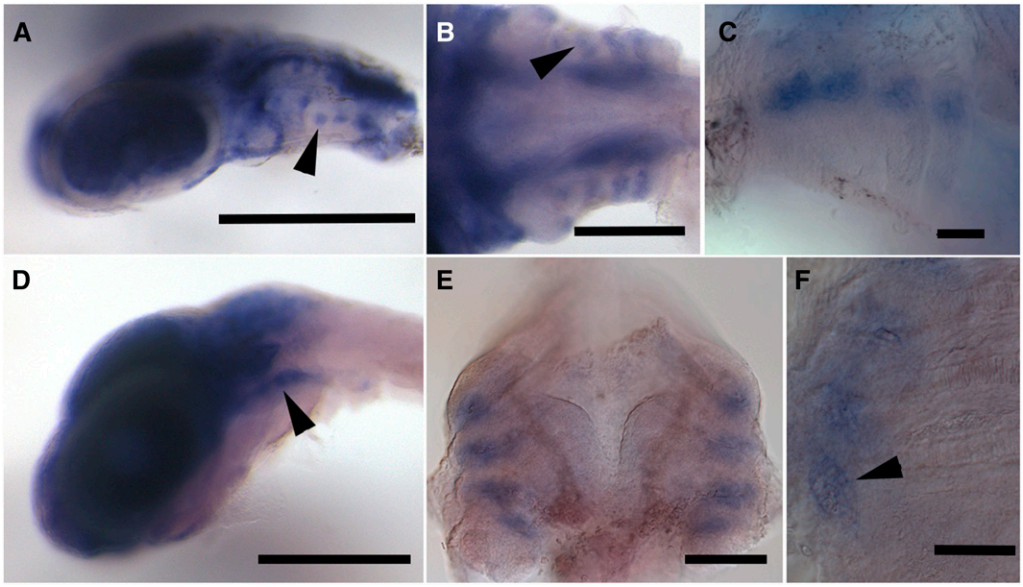

Figure 3 *In situ* hybridization for *Tfap2a*. (A) Lateral view of a 4 dpf embryonic head. *Tfap2a* expression in dorsal pharyngeal arch postmigratory cranial neural crest is indicated with an arrowhead. (B) Ventral view of a 5 dpf embryo; arrowhead indicates pharyngeal arch expression. (C) Ventrolateral view of a 5 dpf embryo; *Tfap2a* expression is visible at the dorsal ends of the pharyngeal pouches. (D) Lateral view of 7 dpf embryo. *Tfap2a* expression remains in the dorsal pharyngeal arches (arrowhead). (E) Dorsal view of a dissected 7 dpf branchial skeleton. (F) Higher magnification of dorsal view of 7 dpf branchial skeleton. Arrowhead indicates expression in condensing epibranchial mesenchymal cells. Scale bars: A and D = 500 μm; B = 200 μm; C, E, and F = 100 μm. A–D show the anterior on the left; E and F show the anterior at the top.

expected based upon the zebrafish *Tfap2a* mutant phenotype (Holzschuh *et al.* 2003; Knight *et al.* 2003), homozygous mutants with a severe lethal craniofacial phenotype (Figure 5, A and B) were obtained at the expected 25% proportion in each of nine crosses carrying various combinations of the alleles in Table S3. Presence of this phenotype was perfectly concordant with homozygous lesions indicated by loss of a *Pvu*II cut site (see *Materials and Methods*). Homozygous mutant fish were almost entirely lacking a pharyngeal skeleton, while in contrast, the mesodermally derived posterior neurocranium was present and well-formed (Figure 5, C and D). The remnants of the pharyngeal skeletal elements were severely malformed, often asymmetric, and not identifiable (Figure 5, E and F). The branchial skeleton was particularly hypoplastic, and no identifiable ceratobranchial or epibranchial cartilages were present. The craniofacial defects were seen in homozygous mutants in both FTC and LITC genetic backgrounds. Consistent with the known roles of *Tfap2a* in controlling neural crest development and migration (Knight *et al.* 2003, 2004), we also observed severe pigmentation defects in homozygous mutants, including reduced melanophore numbers (Figure 5, G and H). Like the zebrafish *lockjaw* mutant (Knight *et al.* 2004), xanthophores appeared unaffected and iridophores were reduced in homozygous mutant fish (Figure S7).

Because we could not study branchial bone length in homozygous mutants, we outcrossed heterozygotes to wild-type fish to compare bone length in wild-type and heterozygous siblings. We grew fish to ~4 weeks postfertilization (~10 mm standard length, a stage just after the effect of the chromosome 21 branchial bone length QTL could first be detected in the FTC × LITC cross) (Erickson *et al.* 2014). For the *Tfap2a* mutations in the FTC background, we found that EB1 length was slightly but significantly decreased in heterozygous fish (Figure 6A), while surprisingly, the third, fourth, and fifth ceratobranchials (CB3, CB4, and CB5) were slightly but significantly increased (Figure S8). However, in the LITC background, none of the branchial bones measured (CB1–5 and EB1) were significantly different between wild-type and heterozygous fish (Figure 6B and Figure S8). Although our allele specific expression data predict that reducing *Tfap2a* function might lead to an increase in branchial bone length, our functional data suggest that halving the dosage of *Tfap2a* on a freshwater genetic background can both increase (for ventral posterior ceratobranchials) and decrease (for dorsal EB1) branchial bone length.

Discussion

Genetic dissection of a supergene involved in parallel evolution

Many putatively pleiotropic QTL affecting traits of evolutionary, economic, and biomedical interest have been discovered (Feitosa *et al.* 2006; Hall *et al.* 2006; Ookawa *et al.* 2010; Stearns 2010; Saatchi *et al.* 2014), but determining whether the underlying causative loci are the same or different remains a challenge (Wagner and Zhang 2011; Paaby and Rockman 2013). Using recombinant mapping in two genetic crosses, we show that two separate but tightly linked genes, *Bmp6* and *Tfap2a*, form a supergene that increases both the length of bones and the number of teeth in the stickleback branchial skeleton in two freshwater populations. Clustering

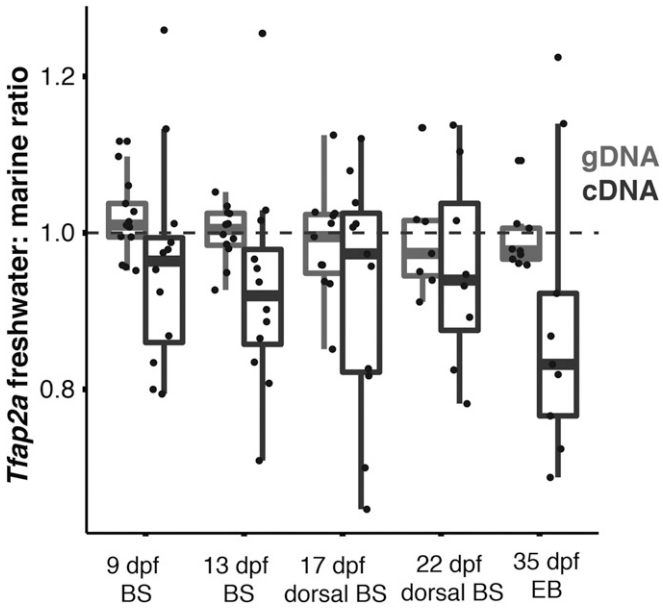

Figure 4 Allele-specific expression of *Tfap2a*. A SNP within exon 2 of *Tfap2a* was amplified by PCR from genomic DNA (gDNA) and by RT-PCR from cDNA collected from ~12 individuals from the PAXB × LITC cross at each of five stages: 9 and 13 dpf branchial skeleton (BS), 17 and 22 dpf dorsal BS, and 35 dpf EB1 tissue. The freshwater/marine allele ratio was calculated for each individual, and the gDNA ratio was compared to the cDNA ratio for each time point by Mann–Whitney *U*-test. While only one developmental stage was significant (9 dpf: $W = 43$, $P = 0.06$; 13 dpf: $W = 35$, $P = 0.03$; 17 dpf: $W = 50$, $P = 0.51$; 22 dpf: $W = 21$, $P = 0.46$; 35 dpf: $W = 18$ $P = 0.05$), collectively the reduced expression of the freshwater allele across the entire data set was highly significant ($W = 851$, $P = 0.001$).

of adaptive loci is predicted by population genetic theory when migration occurs between differentially adapted populations (Yeaman 2013), such as occurs between marine and freshwater adapted sticklebacks (Schluter and Conte 2009; Bell and Aguirre 2013). Migration could maintain close genetic linkage of two alleles affecting trophic morphology, which in turn could facilitate rapid adaptation to freshwater diets upon colonization of new habitats. After the causative mutation(s) for both QTL have been determined, testing for linkage disequilibrium of these alleles in wild marine and estuarine populations could test this hypothesis.

While no study has directly tested whether tooth number or bone length are under selection in freshwater stickleback populations, the causative mutations (once found) could be tested for genomic signatures of selection. It is possible that the mutations underlying only one or neither of these phenotypes are under selection, and that they are instead hitchhiking with other adaptive mutations. The bone length QTL is either not fixed in the FTC population or is dependent upon interactions at other loci, and the ENOB population has a tooth number QTL on chromosome 21 (Erickson *et al.* 2016b) but not a bone length QTL, suggesting that the two elements of this supergene are genetically separable and do not always covary in the wild. The alleles may be maintained at low frequency in marine populations, allowing for repeatable genetic evolution upon freshwater colonization. Alternatively, genetic and developmental constraints may have led to the independent evolution of these craniofacial QTL in multiple populations. The presence and absence of this bone length QTL could be leveraged in future studies to identify polymorphisms associated with the QTL.

In addition to separating the loci controlling bone length and tooth number, we also separated the bone length QTL into at least two loci in the FTC freshwater population by identifying a single recombinant chromosome with effects that are significantly different from both marine and freshwater alleles. These data suggest that a portion of the phenotypic effect maps nearer to the coding sequence of *Tfap2a*, and a portion of the phenotypic effect is attributable to a large non-coding region between *Tfap2a* and *Bmp6*. QTL fractionation has also been observed in a variety of other animal and plant systems (Mackay 2004; Yalcin *et al.* 2004; Willis-Owen and Flint 2006; Studer and Doebley 2011; Johnson *et al.* 2012; Linnen *et al.* 2013), suggesting QTL for complex traits might often represent multiple mutations, especially when the underlying gene has many roles in development, such as *Tfap2a*.

Tfap2a as a candidate gene for craniofacial evolution

Our fine mapping and functional results support *Tfap2a* as a candidate for contributing to craniofacial evolution in sticklebacks. *Tfap2a* was initially identified as an activating protein that binds the SV40 viral enhancer to promote transcription (Williams *et al.* 1988) and has roles in both activating and inhibiting gene expression (Mitchell *et al.* 1987; Williams and Tjian 1991; Gaubatz *et al.* 1995; Pfisterer *et al.* 2002; Eckert *et al.* 2005). During vertebrate embryogenesis, *Tfap2a* is expressed in a variety of tissues in both mice and zebrafish (Mitchell *et al.* 1991; Thisse *et al.* 2001), including the neural crest, an embryonic migratory cell population that gives rise to a variety of tissues, including the pharyngeal skeleton and pigment cells (Bronner and LeDouarin 2012; Mayor and Theveneau 2013). Further studies found a critical role for *Tfap2a* as a master regulator of neural crest development (de Crozé *et al.* 2011; Rada-Iglesias *et al.* 2012). Mice and zebrafish with loss-of-function mutations have severe craniofacial defects (Schorle *et al.* 1996; Zhang *et al.* 1996; Holzschuh *et al.* 2003; Knight *et al.* 2003, 2004) likely due to *Tfap2a*'s role in the pharyngeal ectoderm (Knight *et al.* 2005). Conditional knockout of *Tfap2a* in the frontonasal prominence of mice results in a failure of craniofacial outgrowth during postnatal development (Nelson and Williams 2004), while conditional knockout of *Tfap2a/b* in cranial neural crest cells results in a loss of the jaw hinge and other craniofacial phenotypes (Van Otterloo *et al.* 2018). In humans, familial mutations in *Tfap2a* cause branchio-oculo-facial syndrome (Milunsky *et al.* 2008; Stoetzel *et al.* 2009; Tekin *et al.* 2009). Thus, *Tfap2a* plays complex roles at multiple stages of craniofacial development in vertebrates, consistent with the possibility of *cis*-regulatory changes contributing to evolved branchial bone length differences in freshwater sticklebacks.

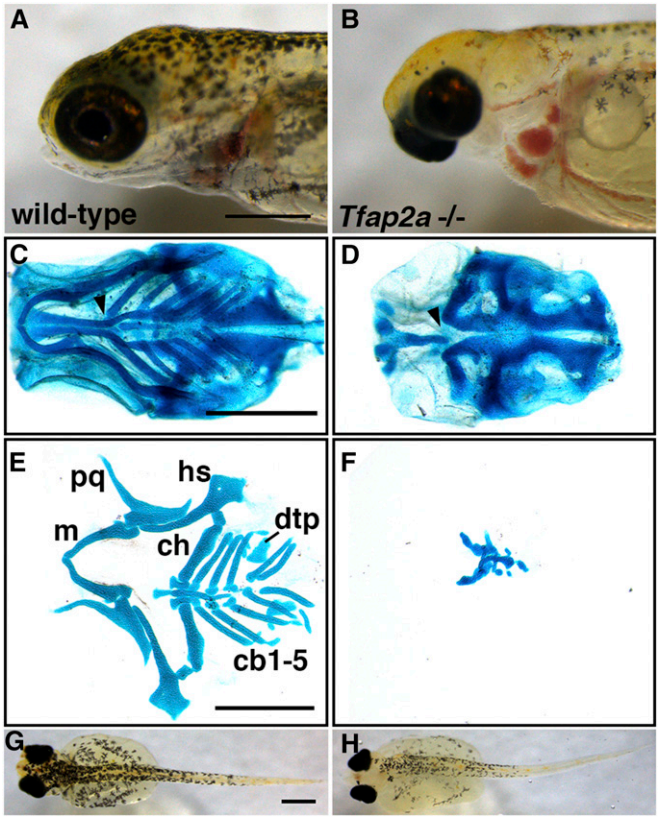

Figure 5 Induced homozygous mutations in *Tfap2a* result in severe craniofacial defects and reduced pigmentation. Wild-type FTC freshwater (A, C, E, and G) and homozygous *Tfap2a* mutant sibling fish (B, D, F, and H). (A and B) Relative to wild-type (A), mutants (B) have severely hypoplastic craniofacial tissue that results in an inability to feed. (C and D) Ventral view of the heads of Alcian blue stained fish reveal defects to the anterior neurocranium in mutant fish (arrowheads). (E and F) Flat-mounted, Alcian blue-stained pharyngeal arch cartilage elements. The remnant cartilages in the mutants are unidentifiable. (G and H) Dorsal views of 9 dpf larvae showing reduced melanophore pigmentation in *Tfap2a* mutants. While FTC fish are shown here, no obvious differences were observed between FTC$^{-/-}$ and LITC$^{-/-}$ fish. Anterior is to the left for all images; scale bar = 500 μm. cb, ceratobranchial; ch, ceratohyal; dtp, dorsal tooth plate; hs, hyosymplectic; m, Meckel's cartilage (lower jaw); pq, palatoquadrate.

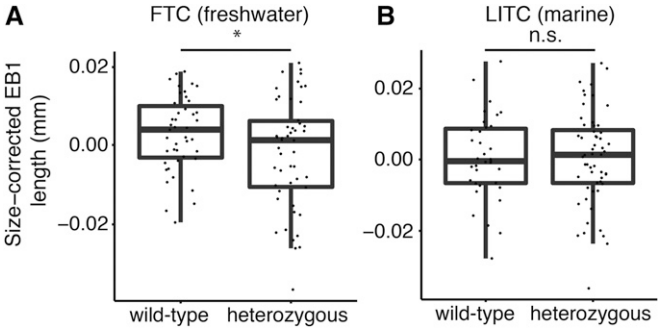

Figure 6 Heterozygous loss of *Tfap2a* produces slightly but significantly shorter EB1 bone length in freshwater, but not marine fish. (A) FTC freshwater fish (25–28 dpf) heterozygous for predicted *Tfap2a* loss-of-function mutations have significantly shorter first epibranchial (EB1) length relative to wild-type siblings (*t*-test: $t = 1.99$, d.f. = 87.1, $P = 0.049$, asterisk). (B) LITC marine heterozygous *Tfap2a* mutant fish have no significant difference in EB1 length compared to wild-type siblings. Additional bone length phenotypes are shown in Figure S8. There was no difference in standard length between +/+ and +/− fish in either population ($P > 0.5$). EB1 length is size-corrected for standard length; residuals are shown.

Evolved differences in neural crest cell regulation and patterning are hypothesized to underlie craniofacial evolution in primates, birds, and cichlids, as well as the domestication of a variety of mammals (Fish *et al.* 2014; Powder *et al.* 2014; Wilkins *et al.* 2014; Prescott *et al.* 2015). Therefore, *Tfap2a* might affect stickleback branchial bone length by altering the early specification and patterning of cranial neural crest cells that eventually form the pharyngeal skeleton. Consistent with this possibility, we observed tissue-restricted expression of *Tfap2a* in dorsal postmigratory cranial neural crest in developing pharyngeal arches, as well as later in development in the primordia of stickleback branchial bones. *Tfap2a* might regulate dorsal branchial skeleton morphology by modifying the dorsal–ventral partitioning of cells within the pharyngeal arches. The *cis*-regulatory differences in freshwater *Tfap2a* expression might reflect spatial and/or quantitative changes in *Tfap2a* expression, which could be tested once *Tfap2a* enhancers of craniofacial expression are determined. While conserved regulatory elements of *Tfap2a* have been described in mice (Zhang and Williams 2003; Donner and Williams 2006; Feng *et al.* 2008), an enhancer driving pharyngeal arch neural crest has not been reported. Future genomic sequence comparisons and transgenic assays could identify additional enhancers driving expression in pharyngeal arch neural crest (including the precursors of the EB1 studied here). In addition to possible changes in pharyngeal arch neural crest regulatory elements, it is also possible that the synonymous change identified here contributes to or even fully explains the observed allelic expression differences through differences in mRNA processing or stability, both of which could also contribute to the observed allele-specific difference in transcript abundance.

In addition to its roles in craniofacial development, *Tfap2a* also regulates the differentiation and maintenance of cell types important for skeletal development. *Tfap2a* mutant mice and chimeric mice have partially penetrant absence of zeugopods and polydactyly (Schorle *et al.* 1996; Zhang *et al.* 1996; Nottoli *et al.* 1998). During mammalian long bone development, analogous to fish branchial bone development (Haines 1942), an initial cartilage template for the bone is formed. Osteoblasts then secrete bone matrix surrounding this template, but a region of cartilage cells (chondrocytes) is left behind at either end as a growth plate for further bone elongation (Kronenberg 2003; Hall 2005; Karsenty *et al.* 2009). TFAP2A protein is expressed in the growth plate of mouse long bones (Davies *et al.* 2002), is thought to regulate a variety of genes related to chondrocyte development (Xie *et al.* 1998; Tuli *et al.* 2002), and is a negative regulator of chondrocyte differentiation *in vitro* (Huang *et al.* 2004).

Therefore, a downregulation or reduced function of *Tfap2a* in freshwater fish might cause an increase in chondrocyte differentiation, resulting in greater long bone growth. The allele specific expression of *Tfap2a* seen during early bone development, combined with the manifestation of the bone length QTL observed in juveniles, suggests that some combination of *Tfap2a*'s roles in neural crest development as well as chondrocyte differentiation might underlie the evolved increases in bone length. Furthermore, the fractionation of the QTL in the FTC cross suggests that at least two regions surrounding *Tfap2a*, and possibly two developmental functions, contribute to the evolved phenotypes.

Surprisingly, the effect of *Tfap2a* mutation was more severe in sticklebacks than in zebrafish. While zebrafish *lockjaw* mutants still have identifiable pharyngeal cartilage elements in the jaw and branchial skeleton (Knight *et al.* 2003), stickleback larvae homozygous for *Tfap2a* mutations had only a few severely hypoplastic and unidentifiable pharyngeal skeletal elements, as well as defects in the anterior neurocranium. The remaining chondrocytes appear to be well developed in mutant fish, so the primary craniofacial defect appears to be pharyngeal arch patterning, not cartilage differentiation. Therefore, compared to zebrafish, sticklebacks may have fewer redundant functions of other genes with *Tfap2a* during craniofacial development.

We found that while induced mutations in *Tfap2a* caused lethal craniofacial defects, heterozygous loss of *Tfap2a* was sufficient to alter branchial bone length in the FTC freshwater background. Based on our ASE data, we predict that freshwater fish likely have lower levels of *Tfap2a*, so they may be more sensitive to reductions in *Tfap2a* function than marine fish. FTC fish heterozygous for mutations in *Tfap2a* had slightly but significantly shorter dorsal (EB1) bones, but significantly longer ventral (CB5) bones. These opposite results suggest that *Tfap2a* could play some role in allocating cells to dorsal and ventral pharyngeal elements, but also suggest that branchial skeleton morphology can be sensitive to *Tfap2a* dosage in a genetic background-specific manner, perhaps similar to the quantitative craniofacial phenotypes reported in heterozygous *Tfap2a* mutant mice (Green *et al.* 2015). The predicted strong loss-of-function mutations generated by TALENs likely do not fully recapitulate *cis*-regulatory mutations in *Tfap2a* that occur in nature, which may affect the timing, location, and/or level of gene expression.

Cis-regulatory changes and morphological evolution

Evolution of *cis*-regulatory modules is thought to be an important general feature of morphological evolution (Stern 2000; Carroll 2008). Because developmental regulatory genes are often expressed and required in a wide variety of tissues at time points throughout development, changes to their regulation, rather than changes to their coding sequences, may prevent deleterious pleiotropic effects. Both *Tfap2a* and *Bmp6* are expressed dynamically in multiple tissues during development (Cleves *et al.* 2014; Erickson *et al.* 2015 and this study) and can have deleterious and lethal loss-of-function phenotypes (P. Cleves, J. Hart, R. Agoglia, M. Jimenez, P. Erickson, L. Gai, and C. Miller, unpublished data, and this study). Here, we provide evidence that a subtle regulatory difference in *Tfap2a* is associated with evolved skeletal changes related to dietary adaptation, but we cannot exclude the possibility that a long distance regulatory element of another gene outside the eight-gene interval (including *Bmp6*) could underlie at least part of the QTL effect (Montavon *et al.* 2011; Marinić *et al.* 2013; Smallwood and Ren 2013; Anderson and Hill 2014). However, the paralogous tightly linked *Tfap2c* and *Bmp7* genes in mice have been found to be in distinct topologically associating domains, suggesting that their regulatory elements are largely distinct (Tsujimura *et al.* 2015).

In the stickleback genome (Jones *et al.* 2012; Glazer *et al.* 2015), *Tfap2a* and *Bmp6* are separated by a large gene desert that is replete with conserved noncoding sequence. These many putative regulatory elements might provide fodder for *cis*-regulatory changes controlling evolved morphological differences. Regulatory changes to other developmental signaling molecules have also been implicated in stickleback evolution (Colosimo *et al.* 2005; Miller *et al.* 2007; Chan *et al.* 2010; Indjeian *et al.* 2016; Ishikawa *et al.* 2017), suggesting that changes to gene regulation may be used to fine-tune developmental processes to produce novel and ecologically beneficial phenotypes. Interestingly, our studies indicate evolved increases in both branchial bone length and pharyngeal tooth number in freshwater stickleback are associated with *cis*-regulatory reductions in expression (Cleves *et al.* 2014). Combined, these findings suggest that evolved gain traits may make "more from less": constructive morphological phenotypes may commonly evolve from mutations that reduce function and/or expression of genes that repress tissue growth (*e.g.*, inhibit tooth replacement or repress chondrocyte differentiation).

Acknowledgments

We thank Monica Jimenez for assistance in designing the *Tfap2a* TALENs, Alyson Smith for assistance in cartilage phenotyping, and Andrew Glazer for identifying polymorphic indels and for helpful discussions on the ASE assay development. This work was funded in part by National Institutes of Health (NIH) grant R01 #DE021475 (C.T.M.), NIH predoctoral training grants #5T32GM007127 (P.A.E.) and # 5T32HG000047-15 (J.C.H.), and the National Science Foundation Graduate Research Fellowship (P.A.C.). Experiments in this study used the Vincent J. Coates Genomics Sequencing Laboratory at University of California, Berkeley, supported by NIH S10 instrumentation grants S10RR029668 and S10RR027303.

Literature Cited

Anderson, E., and R. E. Hill, 2014 Long range regulation of the *sonic hedgehog* gene. Curr. Opin. Genet. Dev. 27: 54–59. https://doi.org/10.1016/j.gde.2014.03.011

Anker, G. C., 1974 Morphology and kinetics of the head of the stickleback, *Gasterosteus aculeatus*. Trans. Zool. Soc. London 32: 311–416.

Balic, A., and I. Thesleff, 2015 Tissue interactions regulating tooth development and renewal, pp. 157–186 in *Current Topics in Developmental Biology, Craniofacial Development*, edited by Y. Chai. Academic Press, New York. https://doi.org/10.1016/bs.ctdb.2015.07.006

Bell, M. A., and W. E. Aguirre, 2013 Contemporary evolution, allelic recycling, and adaptive radiation of the threespine stickleback. Evol. Ecol. Res. 15: 377–411.

Bell, M. A., and S. A. Foster, 1994 *The Evolutionary Biology of the Threespine Stickleback*. Oxford University Press, Oxford, UK.

Bronner, M. E., and N. M. LeDouarin, 2012 Development and evolution of the neural crest: an overview. Dev. Biol. 366: 2–9. https://doi.org/10.1016/j.ydbio.2011.12.042

Carroll, S. B., 2008 Evo-eevo and an expanding evolutionary synthesis: a genetic theory of morphological evolution. Cell 134: 25–36. https://doi.org/10.1016/j.cell.2008.06.030

Cermak, T., E. L. Doyle, M. Christian, L. Wang, Y. Zhang *et al.*, 2011 Efficient design and assembly of custom TALEN and other TAL effector-based constructs for DNA targeting. Nucleic Acids Res. 39: e82. https://doi.org/10.1093/nar/gkr218

Chan, Y. F., M. E. Marks, F. C. Jones, G. Villarreal, M. D. Shapiro *et al.*, 2010 Adaptive evolution of pelvic reduction in sticklebacks by recurrent deletion of a *Pitx1* enhancer. Science 327: 302–305. https://doi.org/10.1126/science.1182213

Cleves, P. A., N. A. Ellis, M. T. Jimenez, S. M. Nunez, D. Schluter *et al.*, 2014 Evolved tooth gain in sticklebacks is associated with a *cis*-regulatory allele of *Bmp6*. Proc. Natl. Acad. Sci. USA 111: 13912–13917. https://doi.org/10.1073/pnas.1407567111

Colosimo, P. F., K. E. Hosemann, S. Balabhadra, G. Villarreal, M. Dickson *et al.*, 2005 Widespread parallel evolution in sticklebacks by repeated fixation of *Ectodysplasin* alleles. Science 307: 1928–1933. https://doi.org/10.1126/science.1107239

Conte, G. L., M. E. Arnegard, C. L. Peichel, and D. Schluter, 2012 The probability of genetic parallelism and convergence in natural populations. Proc. R. Soc. Lond. B Biol. Sci. 279: 5039–5047. https://doi.org/10.1098/rspb.2012.2146

Cowles, C. R., J. N. Hirschhorn, D. Altshuler, and E. S. Lander, 2002 Detection of regulatory variation in mouse genes. Nat. Genet. 32: 432–437. https://doi.org/10.1038/ng992

Davies, S. R., S. Sakano, Y. Zhu, and L. J. Sandell, 2002 Distribution of the transcription factors Sox9, AP-2, and [delta]EF1 in adult murine articular and meniscal cartilage and growth plate. J. Histochem. Cytochem. 50: 1059–1065. https://doi.org/10.1177/002215540205000808

de Crozé, N., F. Maczkowiak, and A. H. Monsoro-Burq, 2011 Reiterative AP2a activity controls sequential steps in the neural crest gene regulatory network. Proc. Natl. Acad. Sci. USA 108: 155–160. https://doi.org/10.1073/pnas.1010740107

Donner, A. L., and T. Williams, 2006 Frontal nasal prominence expression driven by *Tcfap2a* relies on a conserved binding site for STAT proteins. Dev. Dyn. 235: 1358–1370. https://doi.org/10.1002/dvdy.20722

Doyle, E. L., N. J. Booher, D. S. Standage, D. F. Voytas, V. P. Brendel *et al.*, 2012 TAL effector-nucleotide targeter (TALE-NT) 2.0: tools for TAL effector design and target prediction. Nucleic Acids Res. 40: W117–W122. https://doi.org/10.1093/nar/gks608

Eckert, D., S. Buhl, S. Weber, R. Jäger, and H. Schorle, 2005 The AP-2 family of transcription factors. Genome Biol. 6: 246. https://doi.org/10.1186/gb-2005-6-13-246

Ellis, N. A., and C. T. Miller, 2016 Dissection and flat-mounting of the threespine stickleback branchial skeleton. J. Vis. Exp. (111): e54056.

Ellis, N. A., A. M. Glazer, N. N. Donde, P. A. Cleves, R. M. Agoglia *et al.*, 2015 Distinct developmental and genetic mechanisms underlie convergently evolved tooth gain in sticklebacks. Development 142: 2442–2451. https://doi.org/10.1242/dev.124248

Elshire, R. J., J. C. Glaubitz, Q. Sun, J. A. Poland, K. Kawamoto *et al.*, 2011 A robust, simple genotyping-by-sequencing (GBS) approach for high diversity species. PLoS One 6: e19379. https://doi.org/10.1371/journal.pone.0019379

Erickson, P. A., A. M. Glazer, P. A. Cleves, A. S. Smith, and C. T. Miller, 2014 Two developmentally temporal quantitative trait loci underlie convergent evolution of increased branchial bone length in sticklebacks. Proc. R. Soc. Lond. B Biol. Sci. 281: 20140822. https://doi.org/10.1098/rspb.2014.0822

Erickson, P. A., P. A. Cleves, N. A. Ellis, K. T. Schwalbach, J. C. Hart *et al.*, 2015 A 190 base pair, TGF-β responsive tooth and fin enhancer is required for stickleback *Bmp6* expression. Dev. Biol. 401: 310–323. https://doi.org/10.1016/j.ydbio.2015.02.006

Erickson, P. A., N. A. Ellis, and C. T. Miller, 2016a Microinjection for transgenesis and genome editing in threespine sticklebacks. J. Vis. Exp. (111): e54055.

Erickson, P. A., A. M. Glazer, E. E. Killingbeck, R. M. Agoglia, J. Baek *et al.*, 2016b Partially repeatable genetic basis of benthic adaptation in threespine sticklebacks. Evolution 70: 887–902. https://doi.org/10.1111/evo.12897

Farnum, C. E., M. Tinsley, and J. W. Hermanson, 2008a Postnatal bone elongation of the manus *vs.* pes: analysis of the chondrocytic differentiation cascade in *Mus musculus* and *Eptesicus fuscus*. Cells Tissues Organs 187: 48–58. https://doi.org/10.1159/000109963

Farnum, C. E., M. Tinsley, and J. W. Hermanson, 2008b Forelimb *vs.* hindlimb skeletal development in the big brown bat, *Eptesicus fuscus*: functional divergence is reflected in chondrocytic performance in autopodial growth plates. Cells Tissues Organs 187: 35–47. https://doi.org/10.1159/000109962

Feitosa, M. F., T. Rice, K. E. North, A. Kraja, T. Rankinen *et al.*, 2006 Pleiotropic QTL on chromosome 19q13 for triglycerides and adiposity: the HERITAGE family study. Atherosclerosis 185: 426–432. https://doi.org/10.1016/j.atherosclerosis.2005.06.023

Feng, W., J. Huang, J. Zhang, and T. Williams, 2008 Identification and analysis of a conserved *Tcfap2a* intronic enhancer element required for expression in facial and limb bud mesenchyme. Mol. Cell. Biol. 28: 315–325. https://doi.org/10.1128/MCB.01168-07

Fish, J. L., R. S. Sklar, K. C. Woronowicz, and R. A. Schneider, 2014 Multiple developmental mechanisms regulate species-specific jaw size. Development 141: 674–684. https://doi.org/10.1242/dev.100107

Frankel, N., D. F. Erezyilmaz, A. P. McGregor, S. Wang, F. Payre *et al.*, 2011 Morphological evolution caused by many subtle-effect substitutions in regulatory DNA. Nature 474: 598–603. https://doi.org/10.1038/nature10200

Gaubatz, S., A. Imhof, R. Dosch, O. Werner, P. Mitchell *et al.*, 1995 Transcriptional activation by Myc is under negative control by the transcription factor AP-2. EMBO J. 14: 1508–1519.

Glazer, A. M., P. A. Cleves, P. A. Erickson, A. Y. Lam, and C. T. Miller, 2014 Parallel developmental genetic features underlie stickleback gill raker evolution. Evodevo 5: 19. https://doi.org/10.1186/2041-9139-5-19

Glazer, A. M., E. E. Killingbeck, T. Mitros, D. S. Rokhsar, and C. T. Miller, 2015 Genome assembly improvement and mapping convergently evolved skeletal traits in sticklebacks with genotyping-by-sequencing. G3 5: 1463–1472. https://doi.org/10.1534/g3.115.017905

Green, M. R., and J. Sambrook, 2012 *Molecular Cloning : A Laboratory Manual*. Cold Spring Harbor Laboratory Press, Cold Spring Harbor, NY.

Green, R. M., W. Feng, T. Phang, J. L. Fish, H. Li *et al.*, 2015 *Tfap2a*-dependent changes in mouse facial morphology result in clefting that can be ameliorated by a reduction in *Fgf8* gene dosage. Dis. Model. Mech. 8: 31–43. https://doi.org/10.1242/dmm.017616

Gross, H. P., and J. M. Anderson, 1984 Geographic variation in the gillrakers and diet of European threespine sticklebacks, *Gasterosteus aculeatus*. Copeia 1984: 87–97. https://doi.org/10.2307/1445038

Haines, R. W., 1934 Epiphyseal growth in the branchial skeleton of fishes. Q. J. Microsc. Sci. 77: 77–97.
Haines, R. W., 1942 The evolution of epiphyses and of endochondral bone. Biol. Rev. Camb. Philos. Soc. 17: 267–292. https://doi.org/10.1111/j.1469-185X.1942.tb00440.x
Hall, B. K., 2005 *Bones and Cartilage: Developmental and Evolutionary Skeletal Biology*. Academic Press, London.
Hall, M. C., C. J. Basten, and J. H. Willis, 2006 Pleiotropic quantitative trait loci contribute to population divergence in traits associated with life-history variation in *Mimulus guttatus*. Genetics 172: 1829–1844. https://doi.org/10.1534/genetics.105.051227
Hermann, K., U. Klahre, M. Moser, H. Sheehan, T. Mandel *et al.*, 2013 Tight genetic linkage of prezygotic barrier loci creates a multifunctional speciation island in *Petunia*. Curr. Biol. 23: 873–877. https://doi.org/10.1016/j.cub.2013.03.069
Holzschuh, J., A. Barrallo-Gimeno, A.-K. Ettl, K. Durr, E. W. Knapik *et al.*, 2003 Noradrenergic neurons in the zebrafish hindbrain are induced by retinoic acid and require *tfap2a* for expression of the neurotransmitter phenotype. Development 130: 5741–5754. https://doi.org/10.1242/dev.00816
Huang, Z., H. Xu, and L. Sandell, 2004 Negative regulation of chondrocyte differentiation by transcription factor AP-2alpha. J. Bone Miner. Res. 19: 245–255. https://doi.org/10.1359/jbmr.2004.19.2.245
Hung, H.-Y., L. M. Shannon, F. Tian, P. J. Bradbury, C. Chen *et al.*, 2012 *ZmCCT* and the genetic basis of day-length adaptation underlying the postdomestication spread of maize. Proc. Natl. Acad. Sci. USA 109: E1913–E1921. https://doi.org/10.1073/pnas.1203189109
Indjeian, V. B., G. A. Kingman, F. C. Jones, C. A. Guenther, J. Grimwood *et al.*, 2016 Evolving new skeletal traits by *cis*-regulatory changes in Bone Morphogenetic Proteins. Cell 164: 45–56. https://doi.org/10.1016/j.cell.2015.12.007
Ishikawa, A., M. Kusakabe, K. Yoshida, M. Ravinet, T. Makino *et al.*, 2017 Different contributions of local- and distant-regulatory changes to transcriptome divergence between stickleback ecotypes. Evolution 71: 565–581. https://doi.org/10.1111/evo.13175
Jeong, S., M. Rebeiz, P. Andolfatto, T. Werner, J. True *et al.*, 2008 The evolution of gene regulation underlies a morphological difference between two *Drosophila* sister species. Cell 132: 783–793. https://doi.org/10.1016/j.cell.2008.01.014
Johnson, E. B., J. E. Haggard, and D. A. St.Clair, 2012 Fractionation, stability, and isolate-specificity of QTL for resistance to *Phytophthora infestans* in cultivated tomato (*Solanum lycopersicum*). G3 2: 1145–1159. https://doi.org/10.1534/g3.112.003459
Jones, F. C., M. G. Grabherr, Y. F. Chan, P. Russell, E. Mauceli *et al.*, 2012 The genomic basis of adaptive evolution in threespine sticklebacks. Nature 484: 55–61. https://doi.org/10.1038/nature10944
Joron, M., R. Papa, M. Beltrán, N. Chamberlain, J. Mavárez *et al.*, 2006 A conserved supergene locus controls colour pattern diversity in *Heliconius* butterflies. PLoS Biol. 4: e303. https://doi.org/10.1371/journal.pbio.0040303
Joron, M., L. Frezal, R. T. Jones, N. L. Chamberlain, S. F. Lee *et al.*, 2011 Chromosomal rearrangements maintain a polymorphic supergene controlling butterfly mimicry. Nature 477: 203–206. https://doi.org/10.1038/nature10341
Karsenty, G., H. M. Kronenberg, and C. Settembre, 2009 Genetic control of bone formation. Annu. Rev. Cell Dev. Biol. 25: 629–648. https://doi.org/10.1146/annurev.cellbio.042308.113308
Kim, K.-W., C. Bennison, N. Hemmings, L. Brookes, L. L. Hurley *et al.*, 2017 A sex-linked supergene controls sperm morphology and swimming speed in a songbird. Nat. Ecol. Evol. 1: 1168–1176. https://doi.org/10.1038/s41559-017-0235-2
Kimmel, C. B., C. T. Miller, G. Kruze, B. Ullmann, R. A. BreMiller *et al.*, 1998 The shaping of pharyngeal cartilages during early development of the zebrafish. Dev. Biol. 203: 245–263. https://doi.org/10.1006/dbio.1998.9016
Kislalioglu, M., and R. N. Gibson, 1977 The feeding relationship of shallow water fishes in a Scottish sea loch. J. Fish Biol. 11: 257–266. https://doi.org/10.1111/j.1095-8649.1977.tb04118.x
Knight, R. D., S. Nair, S. S. Nelson, A. Afshar, Y. Javidan *et al.*, 2003 *lockjaw* encodes a zebrafish *tfap2a* required for early neural crest development. Development 130: 5755–5768. https://doi.org/10.1242/dev.00575
Knight, R. D., Y. Javidan, S. Nelson, T. Zhang, and T. Schilling, 2004 Skeletal and pigment cell defects in the *lockjaw* mutant reveal multiple roles for zebrafish *tfap2a* in neural crest development. Dev. Dyn. 229: 87–98. https://doi.org/10.1002/dvdy.10494
Knight, R. D., Y. Javidan, T. Zhang, S. Nelson, and T. F. Schilling, 2005 AP2-dependent signals from the ectoderm regulate craniofacial development in the zebrafish embryo. Development 132: 3127–3138. https://doi.org/10.1242/dev.01879
Kronenberg, H. M., 2003 Developmental regulation of the growth plate. Nature 423: 332–336. https://doi.org/10.1038/nature01657
Kunte, K., W. Zhang, A. Tenger-Trolander, D. H. Palmer, A. Martin *et al.*, 2014 *Doublesex* is a mimicry supergene. Nature 507: 229–232. https://doi.org/10.1038/nature13112
Küpper, C., M. Stocks, J. E. Risse, N. dos Remedios, L. L. Farrell *et al.*, 2016 A supergene determines highly divergent male reproductive morphs in the ruff. Nat. Genet. 48: 79–83. https://doi.org/10.1038/ng.3443
Lamichhaney, S., G. Fan, F. Widemo, U. Gunnarsson, D. S. Thalmann *et al.*, 2016 Structural genomic changes underlie alternative reproductive strategies in the ruff (*Philomachus pugnax*). Nat. Genet. 48: 84–88. https://doi.org/10.1038/ng.3430
Lemmon, Z. H., and J. F. Doebley, 2014 Genetic dissection of a genomic region with pleiotropic effects on domestication traits in maize reveals multiple linked QTL. Genetics 198: 345–353. https://doi.org/10.1534/genetics.114.165845
Linnen, C. R., Y.-P. Poh, B. K. Peterson, R. D. H. Barrett, J. G. Larson *et al.*, 2013 Adaptive evolution of multiple traits through multiple mutations at a single gene. Science 339: 1312–1316. https://doi.org/10.1126/science.1233213
Lowry, D. B., and J. H. Willis, 2010 A widespread chromosomal inversion polymorphism contributes to a major life-history transition, local adaptation, and reproductive isolation. PLoS Biol. 8: e1000500 (erratum: PLoS Biol. 10 (2012)). https://doi.org/10.1371/journal.pbio.1000500
Mackay, T. F., 2004 The genetic architecture of quantitative traits: lessons from *Drosophila*. Curr. Opin. Genet. Dev. 14: 253–257. https://doi.org/10.1016/j.gde.2004.04.003
Marinić, M., T. Aktas, S. Ruf, and F. Spitz, 2013 An integrated holo-enhancer unit defines tissue and gene specificity of the *Fgf8* regulatory landscape. Dev. Cell 24: 530–542. https://doi.org/10.1016/j.devcel.2013.01.025
Mather, K., 1950 The genetical architecture of heterostyly in *Primula sinensis*. Evolution 4: 340–352. https://doi.org/10.1111/j.1558-5646.1950.tb01404.x
Mayor, R., and E. Theveneau, 2013 The neural crest. Development 140: 2247–2251. https://doi.org/10.1242/dev.091751
McGee, M. D., and P. C. Wainwright, 2013 Convergent evolution as a generator of phenotypic diversity in threespine stickleback. Evolution 67: 1204–1208. https://doi.org/10.1111/j.1558-5646.2012.01839.x
McGee, M. D., D. Schluter, and P. C. Wainwright, 2013 Functional basis of ecological divergence in sympatric stickleback. BMC Evol. Biol. 13: 277. https://doi.org/10.1186/1471-2148-13-277
McGregor, A. P., V. Orgogozo, I. Delon, J. Zanet, D. G. Srinivasan *et al.*, 2007 Morphological evolution through multiple *cis*-regulatory mutations at a single gene. Nature 448: 587–590. https://doi.org/10.1038/nature05988

Miller, C. T., S. Beleza, A. A. Pollen, D. Schluter, R. A. Kittles *et al.*, 2007 *cis*-regulatory changes in *Kit ligand* expression and parallel evolution of pigmentation in sticklebacks and humans. Cell 131: 1179–1189. https://doi.org/10.1016/j.cell.2007.10.055

Miller, C. T., A. M. Glazer, B. R. Summers, B. K. Blackman, A. R. Norman *et al.*, 2014 Modular skeletal evolution in sticklebacks is controlled by additive and clustered quantitative trait loci. Genetics 197: 405–420. https://doi.org/10.1534/genetics.114.162420

Milunsky, J. M., T. A. Maher, G. Zhao, A. E. Roberts, H. J. Stalker *et al.*, 2008 *TFAP2A* mutations result in branchio-oculo-facial syndrome. Am. J. Hum. Genet. 82: 1171–1177. https://doi.org/10.1016/j.ajhg.2008.03.005

Mitchell, P. J., C. Wang, and R. Tjian, 1987 Positive and negative regulation of transcription in vitro: enhancer-binding protein AP-2 is inhibited by SV40 T antigen. Cell 50: 847–861. https://doi.org/10.1016/0092-8674(87)90512-5

Mitchell, P. J., P. M. Timmons, J. M. Hébert, P. W. Rigby, and R. Tjian, 1991 Transcription factor AP-2 is expressed in neural crest cell lineages during mouse embryogenesis. Genes Dev. 5: 105–119. https://doi.org/10.1101/gad.5.1.105

Montavon, T., N. Soshnikova, B. Mascrez, E. Joye, L. Thevenet *et al.*, 2011 A regulatory archipelago controls *Hox* genes transcription in digits. Cell 147: 1132–1145. https://doi.org/10.1016/j.cell.2011.10.023

Murray, J., and B. Clarke, 1976a Supergenes in polymorphic land snails. II. *Partula suturalis*. Heredity 37: 271–282. https://doi.org/10.1038/hdy.1976.87

Murray, J., and B. Clarke, 1976b Supergenes in polymorphic land snails. I. *Partula taeniata*. Heredity 37: 253–269. https://doi.org/10.1038/hdy.1976.86

Nabours, R. K., 1933 Inheritance of color patterns in the grouse locust *Acrydium arenosum* burmeister (Tettigidae). Genetics 18: 159–171.

Nadeau, N. J., C. Pardo-Diaz, A. Whibley, M. A. Supple, S. V. Saenko *et al.*, 2016 The gene *cortex* controls mimicry and crypsis in butterflies and moths. Nature 534: 106–110. https://doi.org/10.1038/nature17961

Nelson, D. K., and T. Williams, 2004 Frontonasal process-specific disruption of *AP-2alpha* results in postnatal midfacial hypoplasia, vascular anomalies, and nasal cavity defects. Dev. Biol. 267: 72–92. https://doi.org/10.1016/j.ydbio.2003.10.033

Nottoli, T., S. Hagopian-Donaldson, J. Zhang, A. Perkins, and T. Williams, 1998 *AP-2*-null cells disrupt morphogenesis of the eye, face, and limbs in chimeric mice. Proc. Natl. Acad. Sci. USA 95: 13714–13719. https://doi.org/10.1073/pnas.95.23.13714

Ookawa, T., T. Hobo, M. Yano, K. Murata, T. Ando *et al.*, 2010 New approach for rice improvement using a pleiotropic QTL gene for lodging resistance and yield. Nat. Commun. 1: 132. https://doi.org/10.1038/ncomms1132

Orr, H. A., 2005 The probability of parallel evolution. Evolution 59: 216–220. https://doi.org/10.1111/j.0014-3820.2005.tb00907.x

Paaby, A. B., and M. V. Rockman, 2013 The many faces of pleiotropy. Trends Genet. 29: 66–73. https://doi.org/10.1016/j.tig.2012.10.010

Peichel, C. L., and D. A. Marques, 2017 The genetic and molecular architecture of phenotypic diversity in sticklebacks. Philos. Trans. R. Soc. Lond. B Biol. Sci. 372: 20150486.

Peichel, C. L., K. S. Nereng, K. A. Ohgi, B. L. E. Cole, P. F. Colosimo *et al.*, 2001 The genetic architecture of divergence between threespine stickleback species. Nature 414: 901–905. https://doi.org/10.1038/414901a

Pfisterer, P., J. Ehlermann, M. Hegen, and H. Schorle, 2002 A subtractive gene expression screen suggests a role of transcription factor AP-2α in control of proliferation and differentiation. J. Biol. Chem. 277: 6637–6644. https://doi.org/10.1074/jbc.M108578200

Powder, K. E., H. Cousin, G. P. McLinden, and R. C. Albertson, 2014 A nonsynonymous mutation in the transcriptional regulator *lbh* is associated with cichlid craniofacial adaptation and neural crest cell development. Mol. Biol. Evol. 31: 3113–3124. https://doi.org/10.1093/molbev/msu267

Pracana, R., A. Priyam, I. Levantis, R. A. Nichols, and Y. Wurm, 2017 The fire ant social chromosome supergene variant Sb shows low diversity but high divergence from SB. Mol. Ecol. 26: 2864–2879. https://doi.org/10.1111/mec.14054

Prescott, S. L., R. Srinivasan, M. C. Marchetto, I. Grishina, I. Narvaiza *et al.*, 2015 Enhancer divergence and *cis*-regulatory evolution in the human and chimp neural crest. Cell 163: 68–83. https://doi.org/10.1016/j.cell.2015.08.036

Rada-Iglesias, A., R. Bajpai, S. Prescott, S. A. Brugmann, T. Swigut *et al.*, 2012 Epigenomic annotation of enhancers predicts transcriptional regulators of human neural crest. Cell Stem Cell 11: 633–648. https://doi.org/10.1016/j.stem.2012.07.006

Rebeiz, M., J. E. Pool, V. A. Kassner, C. F. Aquadro, and S. B. Carroll, 2009 Stepwise modification of a modular enhancer underlies adaptation in a *Drosophila* population. Science 326: 1663–1667. https://doi.org/10.1126/science.1178357

Rohland, N., and D. Reich, 2012 Cost-effective, high-throughput DNA sequencing libraries for multiplexed target capture. Genome Res. 22: 939–946. https://doi.org/10.1101/gr.128124.111

Rosenblum, E. B., C. E. Parent, and E. E. Brandt, 2014 The molecular basis of phenotypic convergence. Annu. Rev. Ecol. Evol. Syst. 45: 203–226. https://doi.org/10.1146/annurev-ecolsys-120213-091851

Saatchi, M., R. D. Schnabel, J. F. Taylor, and D. J. Garrick, 2014 Large-effect pleiotropic or closely linked QTL segregate within and across ten US cattle breeds. BMC Genomics 15: 442. https://doi.org/10.1186/1471-2164-15-442

Salazar, V. S., L. W. Gamer, and V. Rosen, 2016 BMP signalling in skeletal development, disease and repair. Nat. Rev. Endocrinol. 12: 203–221. https://doi.org/10.1038/nrendo.2016.12

Sanger, T. J., E. A. Norgard, L. S. Pletscher, M. Bevilacqua, V. R. Brooks *et al.*, 2011 Developmental and genetic origins of murine long bone length variation. J. Exp. Zoolog. B Mol. Dev. Evol. 316B: 146–161. https://doi.org/10.1002/jez.b.21388

Sanger, T. J., L. J. Revell, J. J. Gibson-Brown, and J. B. Losos, 2012 Repeated modification of early limb morphogenesis programmes underlies the convergence of relative limb length in *Anolis* lizards. Proc. Biol. Sci. 279: 739–748. https://doi.org/10.1098/rspb.2011.0840

Schluter, D., and G. L. Conte, 2009 Genetics and ecological speciation. Proc. Natl. Acad. Sci. USA 106(Suppl. 1): 9955–9962. https://doi.org/10.1073/pnas.0901264106

Schorle, H., P. Meier, M. Buchert, R. Jaenisch, and P. J. Mitchell, 1996 Transcription factor AP-2 essential for cranial closure and craniofacial development. Nature 381: 235–238. https://doi.org/10.1038/381235a0

Schwander, T., R. Libbrecht, and L. Keller, 2014 Supergenes and complex phenotypes. Curr. Biol. 24: R288–R294. https://doi.org/10.1016/j.cub.2014.01.056

Smallwood, A., and B. Ren, 2013 Genome organization and long-range regulation of gene expression by enhancers. Curr. Opin. Cell Biol. 25: 387–394. https://doi.org/10.1016/j.ceb.2013.02.005

Smith, C. M., J. H. Finger, T. F. Hayamizu, I. J. McCright, J. Xu *et al.*, 2014 The mouse Gene Expression Database (GXD): 2014 update. Nucleic Acids Res. 42: D818–D824.

Stearns, F. W., 2010 One hundred years of pleiotropy: a retrospective. Genetics 186: 767–773. https://doi.org/10.1534/genetics.110.122549

Steiner, C. C., J. N. Weber, and H. E. Hoekstra, 2007 Adaptive variation in beach mice produced by two interacting pigmentation genes. PLoS Biol. 5: e219 (erratum: PLoS Biol. 6: e36). https://doi.org/10.1371/journal.pbio.0050219

Stern, D. L., 2000 Perspective: evolutionary developmental biology and the problem of variation. Evolution 54: 1079–1091. https://doi.org/10.1111/j.0014-3820.2000.tb00544.x

Stern, D. L., 2013 The genetic causes of convergent evolution. Nat. Rev. Genet. 14: 751–764. https://doi.org/10.1038/nrg3483

Stern, D. L., and V. Orgogozo, 2008 The loci of evolution: how predictable is genetic evolution? Evolution 62: 2155–2177. https://doi.org/10.1111/j.1558-5646.2008.00450.x

Stoetzel, C., S. Riehm, V. Bennouna Greene, V. Pelletier, J. Vigneron *et al.*, 2009 Confirmation of *TFAP2A* gene involvement in branchio-oculo-facial syndrome (BOFS) and report of temporal bone anomalies. Am. J. Med. Genet. A. 149A: 2141–2146. https://doi.org/10.1002/ajmg.a.33015

Studer, A. J., and J. F. Doebley, 2011 Do large effect QTL fractionate? A case study at the maize domestication QTL *teosinte branched1*. Genetics 188: 673–681. https://doi.org/10.1534/genetics.111.126508

Tekin, M., A. Sırmacı, B. Yüksel-Konuk, S. Fitoz, and L. Sennaroğlu, 2009 A complex *TFAP2A* allele is associated with branchio-oculo-facial syndrome and inner ear malformation in a deaf child. Am. J. Med. Genet. A. 149A: 427–430. https://doi.org/10.1002/ajmg.a.32619

Thisse, B., S. Pflumio, M. Furthauer, B. Loppin, V. Heyer *et al.*, 2001 *Expression of the Zebrafish Genome During Embryogenesis*. ZFIN Direct Data Submission. Available at: https://zfin.org/ZDB-PUB-010810-1.

Thomas, J. W., M. Cáceres, J. J. Lowman, C. B. Morehouse, M. E. Short *et al.*, 2008 The chromosomal polymorphism linked to variation in social behavior in the white-throated sparrow (*Zonotrichia albicollis*) is a complex rearrangement and suppressor of recombination. Genetics 179: 1455–1468. https://doi.org/10.1534/genetics.108.088229

Thompson, M. J., and C. D. Jiggins, 2014 Supergenes and their role in evolution. Heredity 113: 1–8. https://doi.org/10.1038/hdy.2014.20

Tsujimura, T., F. A. Klein, K. Langenfeld, J. Glaser, W. Huber *et al.*, 2015 A discrete transition zone organizes the topological and regulatory autonomy of the adjacent *Tfap2c* and *Bmp7* genes. PLoS Genet. 11: e1004897. https://doi.org/10.1371/journal.pgen.1004897

Tuli, R., M. R. Seghatoleslami, S. Tuli, M. S. Howard, K. G. Danielson *et al.*, 2002 p38 MAP kinase regulation of AP-2 binding in TGF-β1-stimulated chondrogenesis of human trabecular bone-derived cells. Ann. N. Y. Acad. Sci. 961: 172–177. https://doi.org/10.1111/j.1749-6632.2002.tb03077.x

Tuttle, E. M., A. O. Bergland, M. L. Korody, M. S. Brewer, D. J. Newhouse *et al.*, 2016 Divergence and functional degradation of a sex chromosome-like supergene. Curr. Biol. 26: 344–350. https://doi.org/10.1016/j.cub.2015.11.069

Van Otterloo, E., H. Li, K. L. Jones, and T. Williams, 2018 AP-2α and AP-2β cooperatively orchestrate homeobox gene expression during branchial arch patterning. Development 145: dev157438.

Wagner, G. P., and J. Zhang, 2011 The pleiotropic structure of the genotype–phenotype map: the evolvability of complex organisms. Nat. Rev. Genet. 12: 204–213. https://doi.org/10.1038/nrg2949

Wainwright, P. C., 2006 Functional morphology of the pharyngeal jaw apparatus, pp. 77–101 in *Fish Physiology: Fish Biomechanics*. Academic Press, San Diego.

Wang, H., T. Nussbaum-Wagler, B. Li, Q. Zhao, Y. Vigouroux *et al.*, 2005 The origin of the naked grains of maize. Nature 436: 714–719. https://doi.org/10.1038/nature03863

Wang, J., Y. Wurm, M. Nipitwattanaphon, O. Riba-Grognuz, Y.-C. Huang *et al.*, 2013 A Y-like social chromosome causes alternative colony organization in fire ants. Nature 493: 664–668. https://doi.org/10.1038/nature11832

Wenke, A.-K., and A. K. Bosserhoff, 2010 Roles of AP-2 transcription factors in the regulation of cartilage and skeletal development. FEBS J. 277: 894–902. https://doi.org/10.1111/j.1742-4658.2009.07509.x

Wilkins, A. S., R. W. Wrangham, and W. T. Fitch, 2014 The "domestication syndrome" in mammals: a unified explanation based on neural crest cell behavior and genetics. Genetics 197: 795–808. https://doi.org/10.1534/genetics.114.165423

Williams, T., and R. Tjian, 1991 Analysis of the DNA-binding and activation properties of the human transcription factor AP-2. Genes Dev. 5: 670–682. https://doi.org/10.1101/gad.5.4.670

Williams, T., A. Admon, B. Lüscher, and R. Tjian, 1988 Cloning and expression of AP-2, a cell-type-specific transcription factor that activates inducible enhancer elements. Genes Dev. 2: 1557–1569. https://doi.org/10.1101/gad.2.12a.1557

Wills, D. M., C. J. Whipple, S. Takuno, L. E. Kursel, L. M. Shannon *et al.*, 2013 From many, one: genetic control of prolificacy during maize domestication. PLoS Genet. 9: e1003604. https://doi.org/10.1371/journal.pgen.1003604

Willis-Owen, S. A. G., and J. Flint, 2006 The genetic basis of emotional behaviour in mice. Eur. J. Hum. Genet. 14: 721–728. https://doi.org/10.1038/sj.ejhg.5201569

Wittkopp, P. J., B. K. Haerum, and A. G. Clark, 2004 Evolutionary changes in *cis* and *trans* gene regulation. Nature 430: 85–88. https://doi.org/10.1038/nature02698

Xie, W. F., S. Kondo, and L. J. Sandell, 1998 Regulation of the mouse cartilage-derived retinoic acid-sensitive protein gene by the transcription factor AP-2. J. Biol. Chem. 273: 5026–5032. https://doi.org/10.1074/jbc.273.9.5026

Yalcin, B., S. A. G. Willis-Owen, J. Fullerton, A. Meesaq, R. M. Deacon *et al.*, 2004 Genetic dissection of a behavioral quantitative trait locus shows that *Rgs2* modulates anxiety in mice. Nat. Genet. 36: 1197–1202. https://doi.org/10.1038/ng1450

Yan, H., W. Yuan, V. E. Velculescu, B. Vogelstein, and K. W. Kinzler, 2002 Allelic variation in human gene expression. Science 297: 1143. https://doi.org/10.1126/science.1072545

Yeaman, S., 2013 Genomic rearrangements and the evolution of clusters of locally adaptive loci. Proc. Natl. Acad. Sci. USA 110: E1743–E1751. https://doi.org/10.1073/pnas.1219381110

Zhang, J., and T. Williams, 2003 Identification and regulation of tissue-specific cis-acting elements associated with the human AP-2α gene. Dev. Dyn. 228: 194–207. https://doi.org/10.1002/dvdy.10365

Zhang, J., S. Hagopian-Donaldson, G. Serbedzija, J. Elsemore, D. Plehn-Dujowich *et al.*, 1996 Neural tube, skeletal and body wall defects in mice lacking transcription factor AP-2. Nature 381: 238–241. https://doi.org/10.1038/381238a0

Communicating editor: K. Peichel